AJNR

The cochlear nuclear complex: MR location and abnormalities.

S S Gebarski, D L Tucci and S A Telian

AJNR Am J Neuroradiol 1993, 14 (6) 1311-1318
http://www.ajnr.org/content/14/6/1311

The Cochlear Nuclear Complex: MR Location and Abnormalities

Stephen S. Gebarski,[1] Debara L. Tucci,[2] and Steven A. Telian[2]

PURPOSE: To determine the usefulness of MR imaging in locating known structural landmarks of the cochlear nuclear complex (CNC), and to determine the frequency of CNC abnormalities, based on these landmarks, in patients referred for MR evaluation of unilateral sensorineural hearing loss. **SUBJECTS AND METHODS:** We studied 12 consecutive months of temporal bone/posterior fossa MR images retrospectively to find four known structural landmarks of the CNC: the vestibulocochlear nerve root entry zone; the cerebellar flocculus; the curvilinear choroid plexus along and protruding from the foramen of Luschka; and the bulge of the CNC into the lateral recess of the fourth ventricle and the foramen of Luschka. We tabulated the number of landmarks located per CNC and the number and type of CNC MR abnormalities. Medical records were then reviewed to tabulate clinical indication for MR imaging, type of hearing deficit, and etiology of the hearing deficit and clinical-pathologic proof. **RESULTS:** 175 patients (ages 15–75 years) provided 350 CNCs for study. All 350 CNCs showed at least three of the four landmarks. Thirteen of the 175 patients (7.4%) had focal CNC MR abnormalities; 136 of these 175 patients had been referred for MR evaluation of unilateral sensorineural hearing loss. In 10 of these 136 patients (7.4%), the CNC abnormalities shown on MR proved to be the cause of the sensorineural hearing loss. **CONCLUSIONS:** MR reliably delineates the CNC. Over 1 year, approximately 7% of patients referred for MR evaluation of unilateral sensorineural hearing loss had MR-determined focal CNC abnormalities that caused the sensorineural hearing loss.

Index terms: Nerves, vestibulocochlear (VIII); Nerves; magnetic resonance; Nerves, anatomy; Hearing loss

AJNR 14:1311–1318, Nov/Dec 1993

The cochlear nuclear complex (CNC) is a structural and functional unit of the brain stem with well-defined gross anatomic and surgical landmarks (1–7). General magnetic resonance (MR) studies of the brain stem, reviews of acoustic pathway imaging, and studies of less common causes of sensorineural hearing loss (SNHL) discuss the location of the CNC but do not specifically evaluate the ability of MR imaging to locate CNC landmarks in a large number of patients (8–10). Disease frequencies and treatments differ markedly between the CNC and the vestibulocochlear nerve, cranial nerve VIII (CN 8), but CNC lesions can present with unilateral SNHL identical to that seen with lesions of CN 8 (9–12). We designed a retrospective study to determine the usefulness of MR imaging in locating previously reported structural landmarks of the CNC and the frequency of CNC abnormalities shown on MR images in patients referred for an evaluation of unilateral SNHL.

Materials and Methods

We retrospectively studied all patients referred to our institution over 12 consecutive months for temporal bone/posterior fossa MR imaging. MR imaging was performed with a 1.5-T system (Signa, GE Medical Systems, Milwaukee, Wis) using a quadrature head coil. Spin-echo sequences were used to acquire axial images of the temporal bones/posterior fossa at 567/20/2 (repetition time/echo time/excitations), 256 × 192 matrix, 20-cm field of view, and 3.0-mm section thickness with a 0.5-mm intersection gap. This sequence was acquired before and immediately after the intravenous infusion of gadopentetate dimeglumine at 0.1 mmol/kg. Precontrast axial images of the entire brain were also obtained (2500–3000/30–90, 256 × 256 matrix, 20-cm field of view, 5.0-mm section thickness,

Received April 7, 1993; accepted June 16.

Departments of [1]Radiology and [2]Otolaryngology-Head and Neck Surgery, University of Michigan Medical School, Ann Arbor, MI 48109.

Address reprint requests to Stephen S. Gebarski, MD, Department of Radiology, University Hospital B1D530G/0030, 1500 E. Medical Center Drive, Ann Arbor, MI 48109-0030.

AJNR 14:1311–1318, Nov/Dec 1993 0195-6108/93/1406–1311

and a 1-mm intersection gap). Other sequences were acquired, depending on the clinical indications. However, none of these other sequences was formally analyzed for the purposes of our study because they were not uniformly obtained in all of the patients.

Our imaging analysis consisted of subjective examination of the images to locate four previously reported anatomic landmarks of the CNC (1–7): 1) the vestibulocochlear nerve (CN 8) root-entry zone; 2) the cerebellar flocculus; 3) the curvilinear choroid plexus along and protruding from the foramen of Luschka; and 4) the bulge of the dorsal and ventral portions of the CNC into the lateral recess of the fourth ventricle and the foramen of Luschka. Considering the right and left CNCs separately, each landmark was tabulated as either visible or not visible. All MR abnormalities located in and/or distorting each CNC were tabulated.

Medical records of all patients were then reviewed to locate and tabulate the clinical indication for the MR imaging, the type of hearing deficit, and the cause of the hearing deficit and clinical-pathologic proof of this cause.

Results

One hundred seventy-five patients, ages ranging from 15–75 years, were referred for imaging. These 175 patients provided 350 CNCs for analysis. None of the patients received more than one posterior fossa/temporal bone MR study over the 12 consecutive months.

When both gadolinium-enhanced and unenhanced MR images were examined, we found that 296 (85%) of the CNCs had MR delineation of all four anatomic landmarks. The remaining 54 (15%) showed three of four landmarks. The nonvisualized landmark differed among these 54 CNCs. Thirty-five CNCs (10%) showed no clearly defined CN 8 root entry zone. Eleven CNCs (3%) showed discontinuous choroid plexus in the foramen of Luschka. Eight CNCs (2%) showed no clearly defined cerebrospinal fluid (CSF) in the foramen of Luschka to outline the bulge of the CNC. If gadolinium-enhanced MR imaging was excluded from review, the choroid plexus could not be delineated throughout its length in any of the foramina of Luschka.

Thirteen of the 175 patients (7.4%) had focal CNC MR abnormalities. Imaging and clinical information on these patients is summarized in Table 1.

Review of medical records showed that 136 of the 175 patients (78%) had been referred for MR evaluation of unilateral SNHL. In 10 of these 136 patients (7.4%), the CNC abnormalities shown on MR imaging proved to be the cause of the SNHL. Imaging and clinical information on these 10 patients is summarized in Table 1.

Discussion

Lesions causing unilateral SNHL almost always occur within the sensory organ, the cochlea, or the first-order neural ramifications, the vestibulocochlear nerve (CN 8), and/or CNC (11, 12). Lesions peripheral to the cochlea cause conductive hearing loss, whereas lesions in the central auditory pathways rostral to the CNC often cause no hearing loss or more obscure patterns of bilateral SNHL (12).

Until recently, imaging of cochlear lesions was restricted to abnormalities that altered the computed tomographic appearance of the cochlear portion of the bony labyrinth such as congenital anomalies, erosion, fractures, and pathologic mineralization. Various works now exist reporting imaging of abnormalities of the membranous cochlea alone, usually shown by contrast-enhanced MR imaging (13, 14). In addition, cochlear abnormalities usually can be electrodiagnostically differentiated from lesions of CN 8 or the CNC (15). Imaging investigations of CN 8 are numerous, both in the CT and MR literature, because of the relative ease of imaging the common neoplastic causes of dysfunction at this level (9–11). Although mentioned as part of a report of general brain stem imaging and in reviews of numerous causes of SNHL, CNC imaging has not been specifically studied (8–10).

The surface and sectional landmarks of the CNC have been defined anatomically (1–7). Across its entire length, CN 8 cross-sectional dimensions average 3.0 × 1.3 mm (3). CN 8 leaves the internal auditory canal and traverses the cerebellopontine angle cistern, usually descending slightly, to enter the brain stem at the pontomedullary junction on an average of 15 mm from the medial plane somewhat caudal and, on an average, 1.4 mm lateral to the facial nerve (3). Shortly after entering the brain stem, CN 8 travels along the dorsolateral surface of the rostral medulla approximately doubling in thickness to first form the ventral cochlear nucleus, and then the dorsal cochlear nucleus, immediately superficial to the inferior cerebellar peduncle (1). The ventral and dorsal cochlear nuclei cannot be separated by surface or unstained sectional landmarks, but the ventral cochlear nucleus is always ventrolateral to the dorsal cochlear nucleus (6, 7). Accordingly, one can think of them as a CNC with ventral and dorsal poles (4). The CNC is roughly tubular in shape and is contiguous with the root-entry zone of CN 8. The overall length of the CNC is approximately 8 mm, running almost entirely in

TABLE 1: Summary of clinical and imaging information on patients with MR-detectable focal CNC lesions

Patient, Age, Sex	Clinical Indication for MR	Type of Hearing Deficit	CNC Lesion on MR	Cause of Hearing Deficit	Proof of Cause
1. 52 M	Unilateral SNHL	Unilateral SNHL	Infarction	Listeria meningitis and arteritis	CSF culture
2. 82 F	Unilateral SNHL	Unilateral SNHL	Infarction	Vertebral artery atherosclerosis, embolus	Cerebral angio and clinical course
3. 67 M	Unilateral SNHL	Unilateral SNHL	Infarction	Atrial fibrillation, cardiogenic embolus	Autopsy 2 months after MR
4. 37 F	Unilateral SNHL	Unilateral SNHL	Infarction	SLE arteritis	SLE by ARA criteria
5. 39 M	Unilateral SNHL	Unilateral SNHL	Distortion, signal aberration	PICA aneurysm	SNHL abated post-clipping
6. 60 F	Unilateral SNHL	Unilateral SNHL	Distortion	Vertebral artery and PICA dolichoectasia	No other etiology found for SNHL
7. 81 F	Unilateral SNHL	Unilateral SNHL	Enhancing SNHL	Metastatic breast cancer	Autopsy 11 months after MR
8. 52 M	Unilateral SNHL	Unilateral SNHL	Distortion	Hemangioblastoma	Surgical pathology
9. 39 M	Unilateral SNHL	Unilateral SNHL	Mass, siderosis	Hemorrhagic ependymoma	Surgical pathology
10. 40 F	Unilateral SNHL	Unilateral SNHL	Signal aberration	MS	Poser criteria definite MS
11. 0.5 M	Multiple cranial neuropathies	Bilateral asymmetric SNHL	Multiple brain-stem infarcts	Neonatal anoxia	Clinical course
12. 37 F	Atypical facial pain	Bilateral asymmetric SNHL	Signal aberration	MS	Poser criteria definite MS
13. 31 M	Headache, vertigo	None	Distortion	Cerebellar abscess (no hearing deficit)	Surgical pathology

Note.—CNC = cochlear nuclear complex; SNHL = sensorineural hearing loss; angio = angiography; SLE = systemic lupus erythematosus; ARA criteria from Tan et al (17); PICA = posterior-inferior cerebellar artery; MS = multiple sclerosis; Poser criteria from Poser et al (18).

the canthomeatal plane (4). Therefore, in this axial plane, the CNC comprises a curving tubular structure approximately 3 mm thick and 8 mm long.

Surgical landmarks for the CNC have been defined (4, 5). The cisternal portion of CN 8 approaches the pontomedullary junction by first coming in contact with the cerebellar flocculus, which is just rostral to CN 8 here. CN 8 then moves medially and enters the lateral recess of the fourth ventricle forming the CN 8 root-entry zone. Although CN 8 is usually free in the CSF until it enters the pontomedullary junction, in approximately 5% of individuals CN 8 will coalesce with the surface of the pons, and the precise point of penetration will be lost (4). However, even if this is the case, CN 8 will still travel superficially toward the lateral recess of the fourth ventricle covered immediately posteriorly and superiorly by protruding choroid plexus from the lateral recess of the fourth ventricle. Such protrusion of choroid plexus is seen in more than 96% of individuals (16). This choroid plexus extends lushly into the subarachnoid space at the cerebellopontine angle cistern and then thins somewhat as it traverses the lateral recess and the foramen of Luschka to be contiguous with the bulk of the choroid plexus of the fourth ventricle (1). The most reliable surgical landmark for transition of CN 8 into the ventral cochlear nucleus is the tenia of the fourth ventricle (4). This thin, membranous structure is present in slightly less than half of surgical specimens (4). But, even if the tenia is not present, the ventral pole of the CNC forms a discrete bulge into the floor of the lateral recess and distal portion of the foramen of Luschka (4). The CNC then continues medially arching over the inferior cerebellar peduncle and bulging into the floor of the lateral rectus as the dorsal pole of the CNC (1, 4). Using these anatomic/surgical landmarks, investigators successfully marked the CNC in 19 of 20 cadavers (4). Most importantly for imaging correlation, the CNC always forms the dorsal and rostral border of the most rostral portion of the medulla at the pontomedullary junction along the most rostral extent of the CSF-containing foramen of Luschka and lateral recess of the fourth ventricle (1–7). Axial sections rostral to this will be in the pons/middle-cerebellar peduncles and show no foramen of Luschka. Accordingly, the size of the CNC

and its favorable topographic features should allow it to be located reliably with MR.

Summarizing the above-described landmarks, the path of CN 8 through to the CNC can be defined on MR as follows. The nerve bundle containing the cisternal portion of CN 8 is resolved separate from surrounding CSF (Figs 1 and 2A). This nerve bundle descends, in most cases, to approach and blend with the pontomedullary junction just under the protruding cerebellar flocculus. This junction of CN 8 with the brain stem forms the root-entry zone, the first of our four MR landmarks (Figs 1 and 2B). The cerebellar flocculus, the second of our MR landmarks, is sharply defined separate from CSF (Figs 1, 2B, and 2C). If gadolinium is given, curvilinear contrast-enhancing choroid plexus can be followed from the roof of the fourth ventricle along the foramen of Luschka and then protruding from the foramen into the rostral portion of the lateral recess (Figs 1, 2B, and 2C). This curvilinear choroid plexus forms the third of our four MR landmarks. Moving medially from the root-entry zone, a dorsolateral bulge from the rostral portion of the medulla is seen. This portion of the bulge contains the ventral pole of the CNC, as none of the inferior cerebellar peduncle is immediately contiguous with the surface of the brain stem at this point (1, 3–7). Continuing medially along the foramen of Luschka within this bulge, the surface of the brain stem is made up of the dorsal pole of the CNC. The entire CNC bulge forms the fourth of our landmarks (Figs 1, 2B, and 2C). In most cases, a small amount of CSF in the foramen of Luschka will be seen separating the contrast-enhancing choroid plexus from the CNC bulge (Figs 1 and 2C).

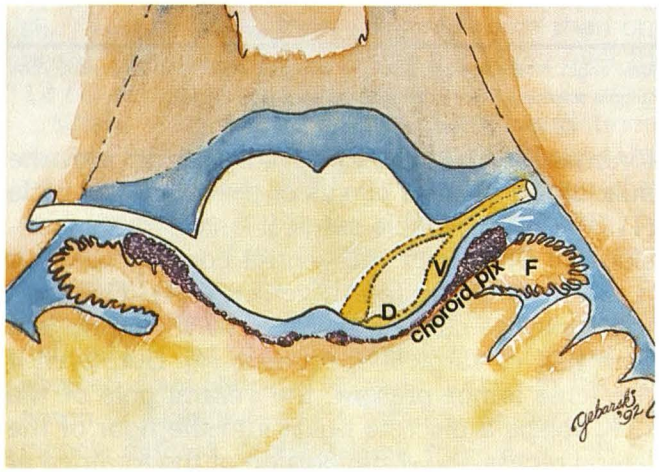

Fig. 1. Axial section of the brain stem at the pontomedullary junction through CN 8 and the foramen of Luschka. Canthomeatal plane of section. CN 8 root-entry zone is seen where the cisternal portion of CN 8 fuses with the brain stem. The vestibular portion of the nerve separates off anteriorly. The cochlear portion of the nerve remains posterior, fusing with the brain stem and forming the ventral portion of the cochlear nuclear complex (*V*). This region of fusion of CN 8 and the brain stem provides the first MR landmark for the CNC, the root-entry zone. The cerebellar flocculus (*F*), the second MR landmark, protrudes into CSF at and about the lateral recess (*white arrow*) of the fourth ventricle. The third MR landmark is the curvilinear choroid plexus (*choroid plx*) extending along the posterior aspect of the foramen of Luschka and protruding into the lateral recess. The fourth MR landmark is the bulge of the dorsal (*D*) and ventral (*V*) portions of the CNC into the choroid plexus and/or CSF in the foramen of Luschka. In the canthomeatal plane, the entire CNC can be included on a single section.

We found that 85% of the CNCs studied demonstrated MR delineation of all four landmarks. The remaining 15% showed three of the four landmarks. No CNC showed fewer than three landmarks. Thirty-five of the CNCs (10%) showed no clearly defined root-entry zone. This is nearly twice the reported incidence of this anatomic variant (4). This is not surprising, because CN 8 could be teased separate from the pia mater in anatomic preparations if CN 8 was simply running along but not penetrating the brain stem. However, MR imaging in such cases would appear to show early fusion of CN 8 with the brain stem. Eleven of the CNCs (3%) showed discontinuous choroid plexus; we could not reliably trace the path of the choroid plexus from the lateral recess all along the foramen of Luschka. This is probably not significant, because all of these CNCs showed CSF intensity outlining the foramen of Luschka. Eight of the CNCs (2%) showed no CSF intensity along the foramen of Luschka. All eight of these were found in younger patients (ages less than 20 years). Younger individuals usually have small ventricles and subarachnoid spaces. However, in all eight of these CNCs, a continuous band of enhancing choroid plexus could be followed along the foramen of Luschka.

We found focal lesions of the CNC in 13 (7.4%) of our 175 patients. Three of these 13 patients had no hearing deficit or more poorly defined bilateral SNHL. They also had MR evidence for additional central-nervous-system lesions distant from the CNC. Final diagnoses on these three were neonatal anoxia with numerous brain stem infarcts, multiple sclerosis, and cerebellar abscess with mass effect on the CNC. A less well-defined clinical presentation of hearing deficit is typical when both first- and higher-order auditory pathways are affected (12).

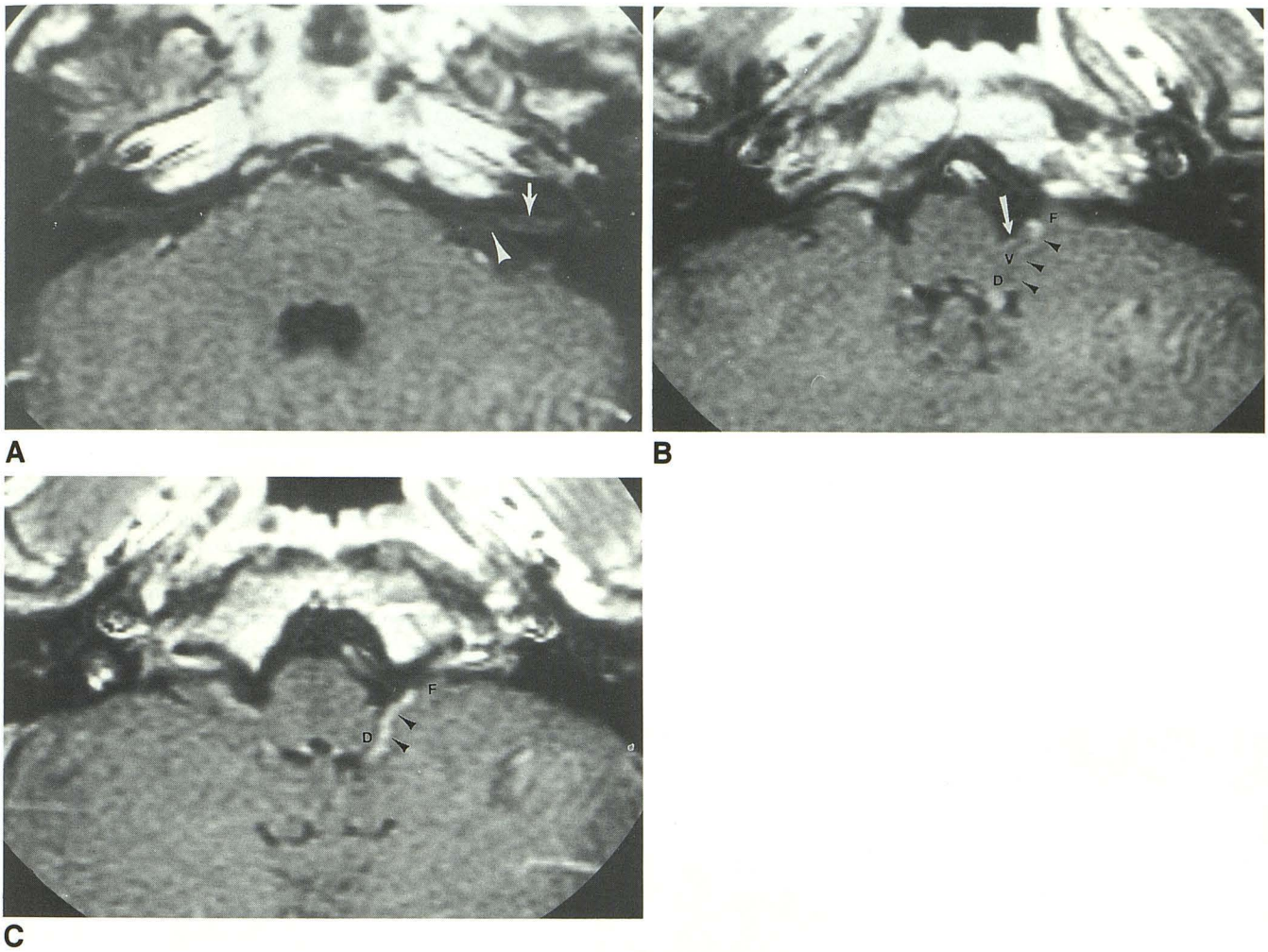

Fig. 2. *A*, Axial MR image (1.5 T, 567/20, 3-mm section thickness) after intravenous infusion of 0.1 mmol/kg of gadopentetate dimeglumine. Inferior orbitomeatal plane of section. Canalicular (*arrow*) and cisternal (*arrowhead*) portions of CN 8 are shown on the *left*. CN 8 descends through the cerebellopontine angle cistern toward the brain stem. No portion of the foramen of Luschka shows on this section.

B, Axial MR image approximately 3 mm caudal to *A*. Cerebellar flocculus (*F*). Choroid plexus (*arrowheads*) extending along the foramen of Luschka and protruding into the lateral recess of the fourth ventricle. *Arrow* represents CN 8 root-entry zone. *D* and *V* represent CNC bulge. When comparing *A* and *B* notice the abrupt transition from the pons/middle cerebellar peduncle to the foramen of Luschka, which contains CSF and choroid plexus. This sudden change in shape and signal makes this landmark easily discernable on both T1- and T2-weighted MR.

C, Axial MR image approximately 3 mm caudal to Fig 3. This section, approximately 3 mm caudal to the root-entry zone of CN 8, shows the most caudal extent of the dorsal (*D*) portion of the CNC. The CNC bulges into a thin band of CSF in the foramen of Luschka. This band of CSF separates the CNC bulge from curvilinear contrast-enhancing choroid plexus (*arrowheads*). The choroid plexus follows the posterior aspect of the foramen of Luschka and bulges into the lateral recess of the fourth ventricle, near the inferior-most aspect of the cerebellar flocculus (*F*). Two adjacent 3-mm sections (*B* and *C*) are needed to include the entire CNC when sectioning in the inferior orbitomeatal plane, which is the most commonly used axial plane for clinical MR imaging.

The remaining 10 of the 13 patients with focal MR imaging abnormalities of the CNC were all from the group of 136 patients referred for MR evaluation of unilateral SNHL. Vascular causes predominated, seen in six of the 10 patients (Figs 3, 4, and 5). There were four cases of CNC infarction, two from arteritis and two from thromboembolism. Vertebral artery and posterior-inferior cerebellar artery abnormalities distorted the CNC in two cases. One of these was dolichoectasia, the other a saccular aneurysm. Neoplasms were the next most common with three cases, one each of metastatic breast cancer (Fig 6), hemangioblastoma, and ependymoma. There was one case of multiple sclerosis (Fig 7).

Although we found no other CNC disease-focused imaging investigations for comparison, two large series include CNC disease along with

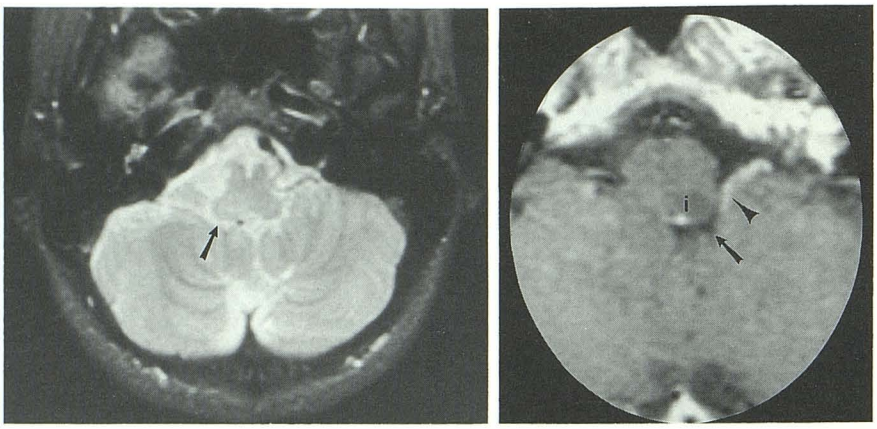

Fig. 3. Axial MR image (1.5 T, 2500/90, 5-mm section thickness), patient three, subacute infarction. Signal aberration and slight swelling involving the right rostodorsal medulla along the foramen of Luschka, defined by the above landmarks as the region of the CNC. *Arrow* indicates CSF in the foramen of Luschka, outlining the CNC bulge. Autopsy 2 months after MR imaging showed infarction involving the CNC.

Fig. 4. Axial contrast-enhanced MR image (1.5 T, 567/20, 3-mm section thickness), patient four, subacute infarction (*i*). Signal aberration and swelling with subtle pathologic contrast enhancement at the edges of the lesion in the left rostrodorsal medulla. Despite the slightly oblique plane of acquisition, CSF (*arrow*) and enhancing choroid plexus (*arrowhead*) in the foramen of Luschka provide reliable landmarks for the CNC.

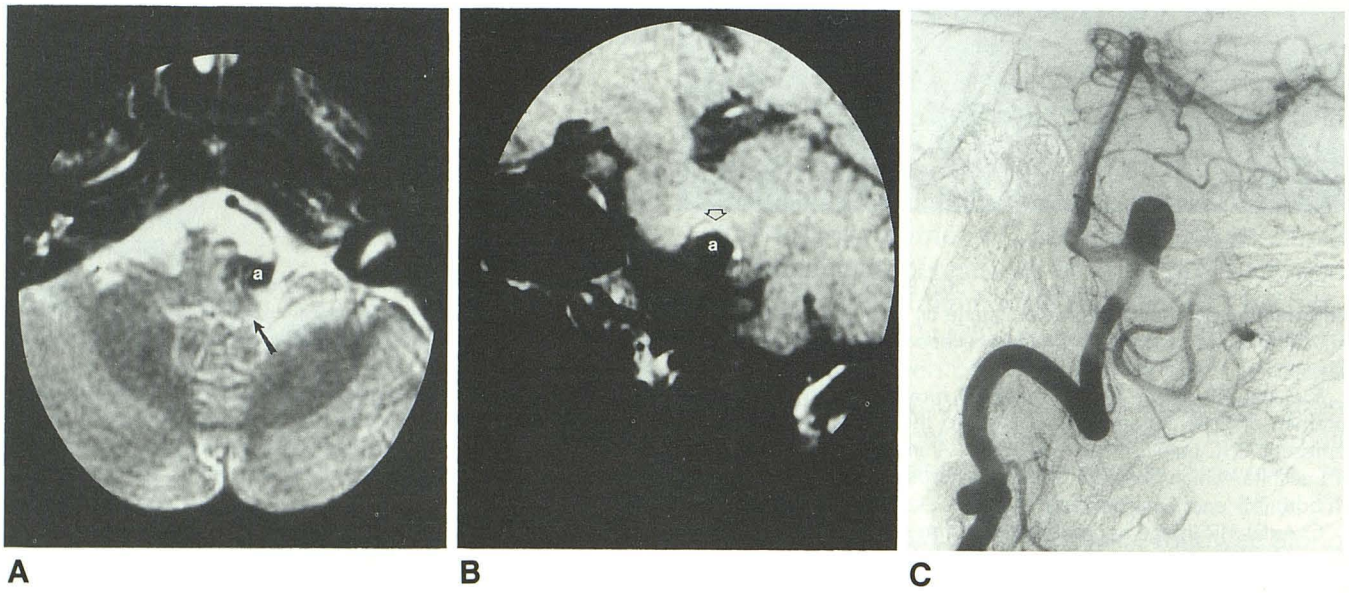

Fig. 5. *A*, Axial MR image (1.5 T, 3000/90, 5-mm section thickness).
B, Sagittal MR image (1.5 T, 500/11, 5-mm section thickness).
C, Detail of subtraction lateral film from left vertebral arteriogram. Patient five, PICA aneurysm (*a*) with subacute hemorrhage (*open arrow*) within the intraluminal thrombus. Focal distortion and signal aberration of the rostrodorsal medulla involving the CNC. Despite the distortion, CSF in the foramen of Luschka (*black arrow*) provides a reliable landmark for the CNC. Although not as useful as the axial plane for delineating the CNC, the sagittal image demonstrates the focal distortion at the pontomedullary junction and affords easy correlation with the arteriogram.

numerous other causes of SNHL (9, 11). If abnormalities of the cochlea and CN 8 are excluded from these previous works, the more recent of these studies reports disease frequencies very similar to ours (9). This work by Armington et al studied 176 patients and showed 11 patients (6%) with vascular disease, five patients (3%) with neoplasm, and six patients (3%) with demyelinating disease. We studied 136 patients with unilateral SNHL and found six patients (4%) with

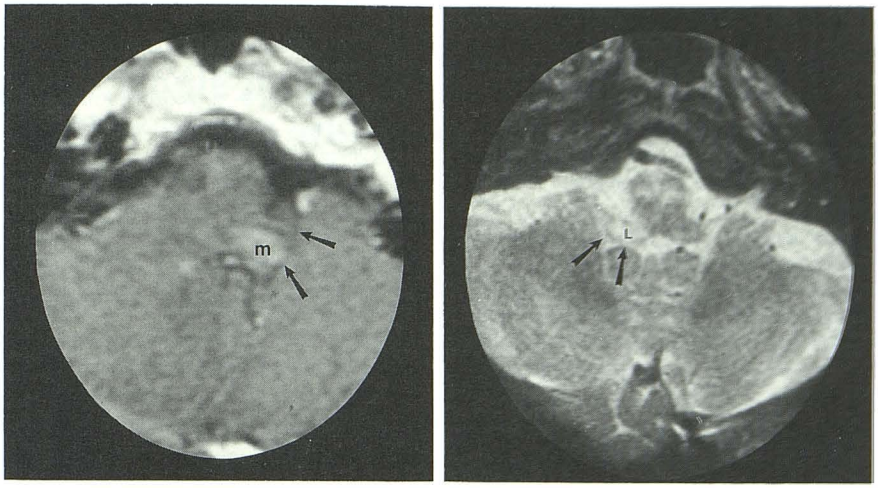

Fig. 6. Axial contrast-enhanced MR image (1.5 T, 567/20, 3-mm section thickness), patient seven, metastatic breast cancer. Contrast-enhancing mass (*m*) expanding the left rostrodorsal medulla. Despite the local distortion and the slight obliquity of the section, CSF in the foramen of Luschka (*arrows*) provides a reliable landmark for the CNC. Autopsy 11 months after MR imaging showed metastatic breast cancer involving the CNC.

Fig. 7. Axial MR image (1.5 T, 3000/90, 5-mm section thickness), patient ten, multiple sclerosis. Lesion (*L*) with intense signal aberration in the right rostrodorsal medulla, mainly in the inferior cerebellar peduncle, but also involving the CNC. Less marked signal aberrations in the left dorsal and bilateral ventral medulla. CSF in the foramen of Luschka (*arrows*) outlines the bulge of the CNC.

vascular disease, three patients (2%) with neoplasm, and one patient (1%) with demyelinating disease.

We reviewed only cases referred for focused posterior fossa/temporal bone MR imaging because we wanted to study reasonably high-resolution images of the CNC in a large number of patients. Clinical selection bias is apparent in our sample, 78% of these patients were referred for an imaging evaluation of unilateral SNHL. Undoubtedly, this selects for more subtle structural lesions, likely raising the number of CNCs showing clearly defined landmarks. However, this is exactly the group of patients where it would seem most useful to carefully look for MR imaging-detectable CNC lesions. Larger lesions most likely would cause other clinical deficits and, because of their size, would be easier to image. The technical quality of our MR imaging was limited by the time constraints of clinical practice and our need for a large number of patients with comparable MR images. The intersection gap, relatively coarse matrix per excitation, and thick sections as well as lack of additional imaging planes all act to reduce resolution and increase partial volume artifact. As is common with clinical MR imaging, our sections were obtained in the inferior orbitomeatal plane. Because of the topographic distribution of the CNC, specialized acquisitions in the canthomeatal plane would be more likely to include the entire CNC on a single section (1–7).

MR imaging reliably delineates the CNC. In addition, our review of 1 year of referrals for MR evaluation of unilateral SNHL shows that approximately 7% of patients had MR-detectable focal CNC abnormalities causing the SNHL. The most common cause was vascular disease, followed by neoplasm and demyelinating disease.

References

1. Carpenter MB. The pons. In: *Human neuroanatomy*. Baltimore: Williams & Wilkins, 1983:363–375
2. Eycleshymer AC, Schoemaker DM. A cross-section anatomy. New York: Appleton-Century-Crofts, 1970:22–29
3. Lang J. Clinical anatomy of the head. New York: Springer-Verlag, 1983:338–351
4. McElveen JT Jr., Hitselberger WE., House WF. Surgical accessibility of the cochlear nuclear complex in man: surgical landmarks. *Otolaryngol Head Neck Surg* 1987;96:135–140
5. Monsell EM., McElveen JT Jr., Hitselberger WE., House WF. Surgical approaches to the human cochlear nuclear complex. *Am J Otol* 1987;8:450–455
6. Terr LI, Edgerton BJ. Surface topography of the cochlear nuclei in humans: two- and three-dimensional analysis. *Hear Res* 1985;17: 51–59
7. Terr LI, Edgerton BJ. Three-dimensional reconstruction of the cochlear nuclear complex in humans. *Arch Otolaryngol* 1985;111: 495–501
8. Bradley WG Jr. MR of the brain stem: a practical approach. *Radiology* 1991;179:319–332

9. Armington WG, Harnsberger HR, Smoker WRK, Osborn AG. Normal and diseased acoustic pathway: evaluation with MR imaging. *Radiology* 1988;167:509–515
10. Mark AS, Seltzer S, Harnsberger HR. Sensorineural hearing loss: more than meets the eye? *AJNR: Am J Neuroradiol* 1993;14:37–45
11. Kumar A, Maudelonde C, Mafee M. Unilateral sensory neural hearing loss: analysis of 200 consecutive cases. *Laryngoscope* 1986;96: 14–32
12. Barbour PJ. A neurologist's approach to a patient with hearing impairment. *Otolaryngol Clin North Am* 1985;18:207–221
13. Mark AS, Seltzer S, Nelson Drake J, Chapman JC, Fitzgerald DC, Gulya AJ. Labyrinthine enhancement on GD-MRI in patients with sudden hearing loss and vertigo: correlation with audiologic and electronystagmographic studies. *Ann Otol Rhinol Laryngol* 1992;101:459–464
14. Seltzer S, Mark AS. Contrast enhancement of the labyrinth on MR scans in patients with sudden hearing loss and vertigo: evidence of labyrinthine disease. *AJNR: Am J Neuroradiol* 1991;12:13–16
15. Kumar A, Mafee M, Torek N. Anatomic specificity of central vestibular signs in posterior fossa lesions. *Ann Otol Rhinol Laryngol* 1982;91:510–515
16. Bradac GB, Simon RS, Fiegler W, Schneider H. A radioanatomic study of the choroid plexus of the fourth ventricle. *Neuroradiology* 1976;11:87–91
17. Tan EM, Cohen AS, Fries JE, et al. The 1982 revised criteria for the classification of systemic lupus erythematosus. *Arthritis Rheum* 1982;25:1271–1277
18. Poser CM, Paty DW, Scheinberg L, et al. New diagnostic criteria for multiple sclerosis: guidelines for research protocols. *Ann Neurol* 1983;13:227–231